Geochimica et Cosmochimica Acta, 1970, Vol. 34, pp. 1053 to 1071. Pergamon Press. Printed in Northern Ireland

Uranium, thorium, potassium and argon in marine phillipsites

MICHEL BERNAT,* RUDOLF H. BIERI, MINORU KOIDE,
JOHN J. GRIFFIN and EDWARD D. GOLDBERG
Scripps Institution of Oceanography, University of California at San Diego
La Jolla, California 92037

(*Received* 23 *April* 1970; *accepted in revised form* 26 *May* 1970)

Abstract—Analyses of elements at trace levels in phillipsites from Pacific Ocean deposits indicate the mineral continues to grow within the sedimentary column. The thorium and uranium concentrations decrease while the mineral concentrations increase with depth in the deposit. This observation can be explained by a continuous growth of the phillipsite within the deposits. The varying concentrations of uranium and thorium in phillipsite, fish teeth and clay minerals from given levels of the core indicate a competition by such substances for the dissolved phases of these elements.

Phillipsites from the surface layers (upper 20 cm) of widely separated deposits have "apparent K–Ar ages" $> 10^6$ yr. Systematic variations in this ratio occur with depth. At three levels a differentiation of the Ar-40/K-40 ratio with respect to size is observed, the larger crystals having smaller ratios and vice versa.

Treatment of three samples with HCl, presumably removing about 40 per cent of the outer layers of the crystals, increased the concentration of radiogenic argon by almost a factor of two. Heating experiments indicate that loss of argon by diffusion is of minor importance.

Idealized models of continuous spherical growth of the mineral over long time intervals, and assuming dr/dt = constant, indicate the time dependence of the Ar-40/K-40 ratios for a growing crystal. Most of the results can be explained by modified versions of such models. Without additional knowledge about the many parameters involved in marine phillipsite formation, however, these minerals are not suitable for dating by the K–Ar method.

INTRODUCTION

THE ZEOLITE phillipsite was initially recognized by MURRAY and RENARD (1891) as a significant component of deep-sea sediments, especially in the Pacific. Occurrences of the mineral are found in those regions characterized by high contributions of volcanic materials and their degradation products and by low inputs of continental debris. It is quite often in association with such marine precipitates as barite, apatite and the ferromanganese minerals, substances that become prominent in slowly accumulating deposits.

Several characteristics of phillipsites and their marine distributions make them attractive as potential time clocks in the marine environment, and these have motivated this investigation. First of all, their thorium concentrations, ranging between 3 and 13 parts per million by weight, have allowed the application of the ionium/thorium technique for the determination of the ages of various strata during the past several hundred thousand years (BERNAT and GOLDBERG, 1969). A continuation of this time record in the phillipsite, using another radioactive technique would be most useful.

The high potassium contents (of the order of 5 per cent, Table 1) in phillipsites suggests an appraisal of their utility as a geochronological tool in the marine sedimentary column in spite of the well known open structures of the minerals. The only

---

[*] Office de la Recherche Scientifique et Technique, Outre-Mer/NATO Fellowship.

data available so far are those of DYMOND (1966) who analyzed phillipsites from 6 different cores. In two cases, where the K–Ar ages of phillipsites can be compared with those from volcanic minerals, a discrepancy of $2\cdot1 \times 10^7$ yr is found. These differences are discussed by DYMOND in terms of mineral formation time and diffusive gas loss during storage at the sea floor and during evacuation procedures prior to extraction.

On the other hand, several disturbing features of phillipsite and its deposition inject a cautionary approach to geochronological considerations. BERNAT and GOLDBERG (1969) suggest that there is a continual growth of phillipsite within the sedimentary column to levels of a million years or so. If this observation is valid, then there can be most undesirable alterations of radioactive time logs. In addition, the phillipsites have open structures which account for their remarkable ion-exchange and molecular sieve properties (STEINFINK, 1962). Such properties may allow exchange of chemical species with those of the aqueous environment and hence may invalidate the assumption of the closed system for the nuclides involved in a given dating scheme.

The goals of this work therefore are to enter into a more systematic study of the factors that control the concentrations of uranium and thorium and to evaluate the potassium–argon method of geochronology for marine phillipsites.

SOME CHARACTERISTICS OF MARINE PHILLIPSITES

Distribution

The highest surface concentrations are in sediments from the Pacific in the vicinity of the mid-Pacific mountains to the north and in the general region of the Society Islands to the south (GOLDBERG, 1961, 1963; BONATTI, 1963). They also occur in Indian Ocean deposits and only rarely are they reported from the Atlantic. In such sediments high concentrations of montmorillonite exist in the clay mineral fractions. Phillipsite is found in calcareous cores. GOLDBERG (1961) reported the highest phillipsite-containing sample on a calcium–carbonate free basis (40 per cent) in a deposit with 21 per cent calcium carbonate. On the other hand, siliceous organic remains rarely survive in phillipsite zones and where they coexist they are heavily corroded.

Chemical composition

The ideal composition is $(K_xNa_{(1-x)})_5Si_{11}Al_5O_{32}\cdot10H_2O$ (STEINFINK, 1962).

Some continental zeolites are characterized by high calcium concentrations in comparison to the much lower values reported for their marine counterparts (Table 1). There are, however, continental zeolites that have the same major element compositions as those of an oceanic origin such as the sample from the zeolitized rhyolite tuff in Nevada (Table 1). There are very few analyses of the minor elements in marine phillipsites. BERNAT and GOLDBERG (1969) report about 10 ppm of thorium as well as a preferential uptake of either protoactinium or actinium, seen as their decay product Th-227, or perhaps both, relative to thorium.

Structure

The structure of a natural marine phillipsite has been determined by STEINFINK (1962) to contain both four and eight membered rings of linked (Si, Al)O_4 tetrahedra

Table 1. Chemical compositions of some marine and continental phillipsites (wt. %)

Element	Pacific Ocean (Goldberg, 1961)	From zeolitized rhyolite tuff, Nevada, U.S.A. (Hay, 1966)*	From tuff, Lake Tecopa, California, U.S.A. (Sheppard and Gude, 1968)	From Basalt Cavity Sicily (Tosto, 1948)
Si	25·0	26·4	26·9	21·5
Mg	0·04	0·25	0·13	0·02
Al	8·8	8·2	7·55	11·6
Ca	0·21	0·29	0·01	2·74
K	5·1	5·1	5·4	3·0
Na	5·5	3·8	3·3	5·6
Ti	0·02	0·17	0·06	n.d.†
P	0·09	0·00	0·00	n.d.†

* Sample contaminated with 5% or less quartz and alkali feldspar as estimated microscopically and by X-ray diffraction analyses.

† Not determined.

with channels running parallel to the (100) and (010) faces. These cavities contain those large cations necessary for electrical neutrality and water molecules. The water molecules apparently can move in and out of the channels with ease without disrupting the linkages of the aluminosilicate framework (Deer *et al.*, 1963).

Ionium/thorium geochronologies and natural radioactive species

The phillipsites in the north Pacific core analyzed by Bernat and Goldberg (1969) maintained the same Th-230/Th-232 values for a given level as did the $<2\ \mu$ fraction or the acid leachate of the sediment sample. This was interpreted as indicating that the thorium isotopes were derived solely from sea water and that there was an insignificant input from detrital minerals. It was inferred that the migration of thorium isotopes within the sediments was minimal.

However, the decreasing concentrations of thorium in the phillipsite that occurred with depth suggested a continuous growth of the mineral with time. The argument was made that the initial formation of phillipsite, at the sediment–water interface, removed most of the thorium from the interstitial solution. Subsequent crystal growth, utilizing dissolved species of such elements as aluminum, silicon, sodium and potassium, from the interstitial water (perhaps these elements dissolved away from the solid components of the deposit, components which put trivial amounts of thorium into solution) results in the decrease of the thorium concentration for the entire mineral. The formation of phillipsite continued for a little over a million years based upon a sedimentation rate of 0·7 mm/1000 years derived from ionium/thorium measurements.

EXPERIMENTAL TECHNIQUES

Uranium and thorium

The separation techniques and the analytical methods are described for thorium isotopes in Bernat and Goldberg (1969).

The phillipsite samples were dissolved in HF to which were added U^{232} and Th^{234} as yield tracers. The Th and U isotopes were isolated through sorption upon an iron hydroxide precipitate. To the dissolved precipitate was added a La carrier and the subsequent LaF_3 precipitate scavenged the Th, leaving the U in solution. The Th isolate was purified with mesityl oxide and TTA extractions and subsequently electroplated following the procedures cited in Bernat and Goldberg (1969).

The supernatant, containing the U, was taken to dryness and dissolved in aqua regia and again taken to dryness. This latter step was repeated once again and the residue was dissolved in 8 N HCl. This solution was passed through an anionic resin (AG1 × 8). The sorbed U was eluted with water. This isolate was purified of any iron by a hexone extraction from a 6 N HCl solution. The U was then electroplated for α spectrometry by the procedure used for Th.

The fish debris were dissolved in HNO_3 to which the U^{232} and Th^{234} tracers were added. The solution was saturated with $Al(NO_3)_3$ and the Th and U extracted into mesityl oxide. The Th and U were taken up in water and the solution was dried.

In order to place all of the uranium in the hexavalent form, the isolate was evaporated to dryness four times with $HClO_4$. Th and U were then taken up in 8 N HCl and the solution passed through an (AG1 × 8) anionic exchange column where the U was retained.

The solution going through the column, which contained the Th, was made 3 N with respect to HCl and passed through the cationic resin and eluted with oxalic acid. It was then electroplated.

In order to check against any tetravalent U being incorporated in the Th isolate, the plated sample, following alpha spectrometric assay, was dissolved and taken to dryness twice with $HClO_4$. The thorium isolation procedure was again carried out. Any differences in activity were attributed to U (IV) and appropriate corrections were made.

The probable errors in the analyses of the fish teeth are ±8 per cent and ±17 per cent for the thorium and uranium respectively.

Potassium and argon

Phillipsite samples were concentrated initially from the cores (Table 2) by sieving (grain sizes greater than 37 μ) followed by magnetic separation. Samples in the less than 37 μ size class were separated into groups by gravitational settling techniques. Subsequent treatments included both heavy liquid and magnetic separations. Purity was ascertained through microscopic examination and X-ray diffraction analyses. The isolated crystals were washed several times with acetone, alcohol and distilled water in an ultrasonic cleaner. This rather elaborate cleaning procedure was found necessary after early analyses with the mass spectrometer showed large contamination by hydrocarbons, phosphorus and chlorine derived from the phillipsite samples.

Table 2. Cores from which phillipsite separates were obtained

Core	Latitude	Longitude	Depth (metres)
LSDH 96	15°10′N	164°39′W	5523
AMPH 113	8°18′S	152°22′W	4837
AMPH 114	9°05′S	151°44′W	5060
AMPH 90	7°30′S	157°41′W	5455
PROA 172	17°21′N	164°12′W	5435
MONSOON 124	26°20′S	156°34′W	5087

Potassium analyses were carried out by atomic absorption or mass spectrometry. Prior sample treatment in the former technique included La–Na borate digestion in the early runs and a fluoboric–boric acid (Bernas, 1968) treatment in the latter ones. The latter technique gave better precision and was used in the majority of the analyses.

The argon was analyzed in the omegatron mass spectrometer. The gas was extracted from the mineral in a furnace especially designed to handle fine-grained samples in milligram amounts (Bieri *et al.*, 1968). Before each extraction an Ar-38 spike was introduced into the furnace volume by a precision metal pipet (Bieri and Koide, 1968). Interferences by hydrocarbons and HCl with the Ar-36 and Ar-38 peaks made the use of a two-stage getter, both stages consisting of Ti-sponge, necessary. After the chemically active gases had been removed by the getters, the sample was expanded into the spectrometer for isotopic analysis of argon.

The validity of the Ar analyses was tested in several ways. First of all, several heating experiments were performed to insure that negligible Ar loss occurred during the time the sample was degassed and the vacuum system pumped down. During pump-down, the vacuum system and furnace were heated to 150°C, but due to conductive heat transfer the samples in the tantalum tubes did not achieve temperatures higher than 50°C, as measured by a thermocouple welded to the tube.

Diffusion experiments show a high degree of variability but indicate that Ar losses at temperatures up to 150°C over time intervals of several hours are negligible (Fig. 1). (Analysis of argon accumulated during an overnight bakeout, with the furnace separated from the pumps, gave the same result.) They also show that the phillipsites hold Ar rather well up to temperatures close to 1000°C. Duplicate runs on some of the samples for which the degassing and preheating (about 50°C) time was varied give reproducible results and also indicate no serious Ar losses during the pretreatment.

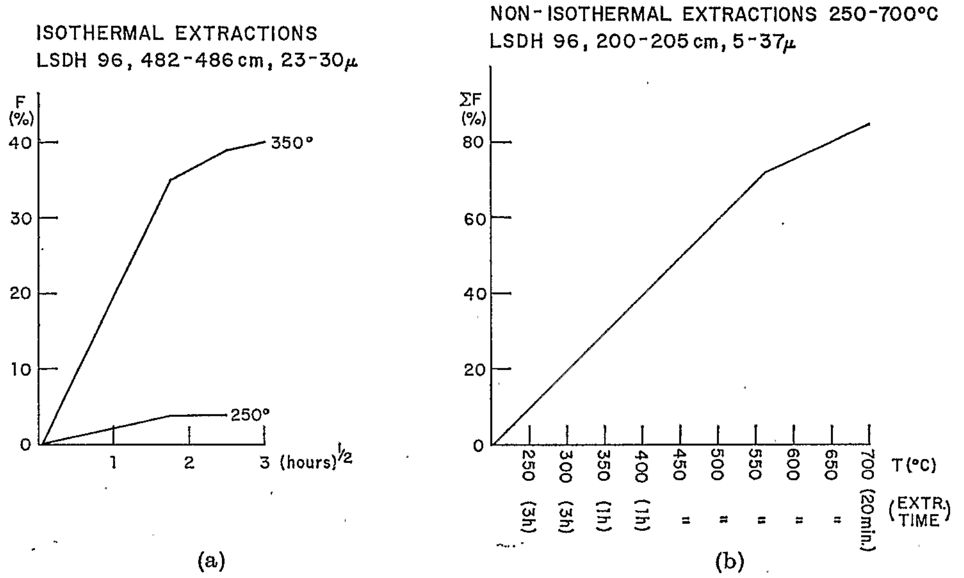

Fig. 1a.

$$F = \frac{\text{amount of } \mathrm{Ar}^{40}_{\mathrm{rad}} \text{ extracted}}{\text{total amount of } \mathrm{Ar}^{40}_{\mathrm{rad}} \text{ in sample}} \times 100$$

vs. square root of time for two different temperatures. Other samples analyzed in the same way suggest large variability.

Fig. 1b. ΣF, the cumulative amount in per cent of radiogenic Ar extracted, as a function of temperature and extraction time.

Total system performance (extraction of the gas, transfer and isotopic analyses) and a calibration of the entire technique was checked with the muscovite sample P-207 from the U.S. Geological Survey (Lanphere and Dalrymple, 1967). The analyses (Table 3) indicate a good precision for the measurement of argon. The P-207 argon concentration published by Lanphere and Dalrymple (1967) is used as the standard in this work.

Leak tests were routinely made during predegassing and just before the extractions. In some cases where the sample analyses showed an unusually high air argon content, a leak check was made in the subsequent analysis, but always with a negative result. Since the omegatron gives well reproducible isotopic ratios, as established in hundreds of air argon analyses, the radiogenic argon concentration in absence of a leak can be ascertained for samples with a radiogenic argon content down to about one per cent.

Table 3. Analyses on Muscovite Standard USGS P-207

Sample size (mg)	Radiogenic Ar (%)	$Ar^{40}_{rad}/Ar^{38}_{spike}$, Normalized to 1 g of sample
13·873	92·7	7821
9·134	84·9	7861
15·753	87·0	7853
17·030	64·0	7824
16·385	67·7	7843
22·240	83·0	7822
20·887	89·3	7849
		Mean 7839 ± 17

Mean radiogenic argon content (LANPHERE *et al.*, 1967): 2·821 ± 0·054 × 10^{-5} cm³ (STP)/g.

Amount of Ar^{38}_{spike} based on this mean and ratio above: 3·599 ± 0·072 × 10^{-8} cm³ (STP).

K concentrations: 8·66, 8·48 and 8·40% (measured). 8·59 ± 0·03% (LANPHERE *et al.*, 1967).

Where contamination of the mass spectrum with hydrocarbons and chlorine occurred, only a range for the radiogenic argon content is given (see, for example, Table 8). Although this problem did not occur with the incorporation of the second getter system, the air–argon problem remained.

The amount of air–argon in an extraction varied from less than 10^{-7} cm³ (STP) to 2 × 10^{-6} cm³ (STP). A large fraction of this derives from the sample itself. The blank produced by heating the sample tubes alone varied from 10^{-8} to 10^{-7} cm³ (STP). Increasing the sample size usually resulted in an increase of the air–argon component. In some cases, however, the extraction furnace clearly contributed a major amount (especially after some of the copper electrodes were replaced). In such analyses, large errors result in the radiogenic argon concentration, but often a lack of sample prevented replicate runs. While this is unfortunate, greater accuracy in such measurements would not alter the conclusions reached in this presentation.

RESULTS

Uranium and thorium

In the cores the thorium and uranium concentrations decrease in the phillipsites while the phillipsite concentrations increase with depth (Tables 4 and 5; Fig. 2). It is difficult to explain these observations by a mechanism other than the continued growth of phillipsite.

A further concern regarding the control of thorium concentrations in phillipsites evolved from the analyses of the Lusiad core where the values were clearly lower (range of 0·65–3·0 ppm) than in the JYN core (range of 3·0–13·2 ppm) previously analyzed (BERNAT and GOLDBERG, 1969).

An explanation may be found in a competition for dissolved thorium species by various mineral surfaces present in the sediment, both authigenic and detrital. To investigate such a probability the thorium isotopes in fish teeth isolated from various levels of LUSIAD 96 and Monsoon 124 were assayed for both uranium and thorium levels as well as for several isotopic ratios of these elements. The results (Table 6) indicate that for both thorium and uranium the fish teeth contain between one and two orders of magnitude higher concentrations than do the zeolites for the same level. Thus, the fish teeth and the phillipsite are two potential repositories for thorium and uranium isotopes. Since the fish teeth have very little thorium and uranium

Table 4. Natural radioactivities and mineralogies in LUSIAD 96G (Gravity Core) and 96P (Piston Core)

Depth (cm)	Uranium (ppm)		Thorium* (ppm)		Th-230/Th-232*		Th-228T/ih-232*		Phillipsite (wt.%)	Clay minerals wt.% in <2 μ size class	
	Total	Phillipsite	Total	Phillipsite	Total	Phillipsite	Total	Phillipsite		Montmorillonite	Illite
					LUSIAD 96 G						
0–3	2·6	0·69	14·8	3·0	9·3	8·0	1·0	14	26		
3–6			12·4	2·5	9·3	8·0	1·0			20	50
8–11	2·9	0·66	6·8	1·6	1·6	3·0	1·0	7	40		
12–15	2·8	0·49	6·4	1·4	1·9	4·0	1·0			75	14
					LUSIAD 96 P						
0–5	3·1	0·46	8·0	2·7(2·8)	4·0	2·3(4·2)	1·0	4·6(7·6)	38	79	14
10–15			7·2	1·8(3·2)	5·5	2·4(1·8)	1·0	6·0(5·7)	33	77	15
20–25		0·59	7·3	1·9(3·3)	4·0	3·7(6·7)	1·0	5·0(6·3)	34	62	27
30–35	3·1	0·46	8·0	2·9(4·3)	1·2	2·8(4·2)	1·0	7·7(5·3)	32	66	23
50–55			7·1	1·6	1·7	1·6	1·0	8·5		92	6
100–105	3·3	0·28	7·3	0·6	1·1	1·6	1·0		53		
151–156	3·3	0·25	6·9	0·9	1·3	1·4			37		
211–216			7·9	0·65	1·1	1·2		10·0		79	14
302–307			8·5	0·79	1·0	0·9		11·0	48		
482–487	3·1	0·32	8·4	0·90	1·1	1·1		9·0	55		
600–605				0·90		1·1		10·0			

* Values in parenthesis are for the greater than 32 μ size fractions whereas values not parenthesized are for the less than 32 μ size fractions. For both the Th-230/Th-232 and the total Th concentrations, the values for the larger size fractions appear to be higher. We have no explanation for this observation.

Table 5. Natural radioactivities and mineralogies in MONSOON 124

Total core			Phillipsite				
Depth (cm)	Th-230/Th-232	Thorium (ppm)	Depth (cm)	Th-230/Th-232	Thorium (ppm)	Phillipsite (wt.%)	Th-228/Th-232
0–4	29·4	18·1	0–6·5	10·0	8·3	6	18
4–6·5	24·5	16·0	10–15	1·4	3·1	11	18
12–16	2·30	13·2	20–25	0·77	3·2	9	19
20–24	1·01	13·1	32–36	0·61		11	14
32–36	0·60	13·8	61–65	0·76	3·2	16	18
61–65	0·56	12·7	96–100	0·60	2·5	15	37
96–100	0·49	12·6			1·4		

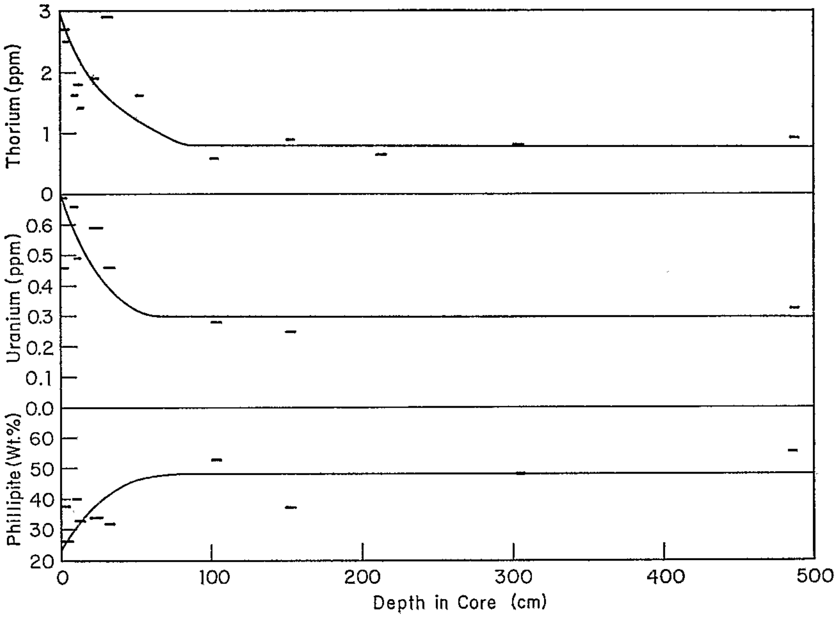

Fig. 2. Uranium, thorium and phillipsite concentrations as a function of depth in LUSIAD 96G and LUSIAD 96P.

while a part of the living organisms, the uptake takes place at the sediment water interface. Otherwise, there would be a continuous increase with depth in the sediment of uranium and thorium in the teeth.

But other mineral involvements for thorium isotopes must exist. For example, the clay mineral analyses on the less than two micron size class of LUSIAD 96 indicate that the upper 6 cm have illite as the dominant clay mineral whereas the lower levels are dominantly montmorillonite (Table 4). The 6 cm level also witnesses a break in thorium concentrations in the total sediment by roughly a factor of 2. Since the clay minerals are a major component of the bulk deposit, it is tempting to relate the change in thorium content to the change in clay mineralogy, with the illites preferentially removing the thorium from sea water. This 6 cm level is also distinguished by a change in color where the first 6 cm are dark yellow, and where the subsequent sections are dark brown.

Table 6. Natural radioactive isotopes in fish teeth

Depth interval (cm)	Uranium (ppm)	Lusiad 96 Thorium (ppm)	Th-230/Th-232	Th-228/Th-232
0–3G	41	209	9·8	0·65
10–15P	33	93	10·0	0·63
0–40P	—	75	14·0	0·88
50–55P	47	60	3·8	1·00
100–105P	49	73	2·7	—
200–205P	42	79	2·1	1·05
360–365P	42	63	2·4	—
600–605P	43	91	1·5	0·73
		Monsoon 124		
10–16	35			—
20–25	36			0·96
32–37	21	230	0·41	—
61–66	25	210	0·64	1·26
96–100	38	200	0·63	0·91

The Th-230/Th-232 ratios are similar in both the bulk sample and in the phillipsite separate for various strata of Lusiad 96. This situation is similar to that previously reported by BERNAT and GOLDBERG (1969) and supports the concept that the behavior of thorium in marine sedimentary processes can be explained by solution chemistry. However, there is a clear disagreement in the ratio between the bulk sample and the phillipsite isolates for materials retrieved near the surface of Monsoon 124 (Table 5). A similar state of affairs was observed in the Th-230/Th-232 ratios recorded in barite and in total sample separates (SOMAYAJULU and GOLDBERG, 1966). These latter results were explained by the differences in the Th-230/Th-232 ratios in the seawaters from which the solid phases received their thorium: the barite obtained this element from waters adjacent to the sediment-water interface; the bulk sample from less deep waters. A model that predicts differences in the Th-230/Th-232 ratios between deep and shallow waters had been proposed previously (GOLDBERG *et al.*, 1964).

In both cores, the phillipsites had markedly higher Th-228/Th-232 ratios than the bulk sediments which possessed the equilibrium values of about 1. This reflects most probably the movement of Ra-228 to the interstitial water following its production from Th-232 in the solid phases and the subsequent uptake by the phillipsite.

Potassium–argon analyses

In K–Ar dating, the age of a specimen is found usually by measuring the concentration of radiogenic argon and of total potassium and then by converting the ratio, $\text{Ar-40}_r/\text{K-40}$,* calculated from the primary information, by

$$\text{Ar-40}_r/\text{K-40} = \frac{\lambda_\varepsilon}{\lambda_\beta + \lambda_\varepsilon}\left(e^{(\lambda_\beta + \lambda_\varepsilon)t} - 1\right) \approx \lambda_\varepsilon t \qquad (1)$$

The approximation is valid as long as the exponential term can be replaced by the first 2 terms of its series expansion with sufficient accuracy. Equation (1) applies when crystal growth occurs over a very short time interval compared to the age of the

---

* Ar-40_r refers to radiogenic argon.

sample, with the crystal acting as a closed system following formation, and with no initial Ar-40 present.

These two conditions, the closed system and the knowledge of initial Ar-40, may not be valid for authigenic minerals formed at the ocean bottom. Evidence has recently been presented by BERNAT and GOLDBERG (1969) that phillipsites may be growing over periods of 10^6 yr. Since little is known about the conditions which govern phillipsite growth in the marine environment, the relation between the Ar/K ratio and time for growth must be considered by simple models. For example, we can assume spherical growth for a nucleus of negligible volume (and hence negligible K and radiogenic Ar content) at time zero. The rate of accretion is chosen to be proportional to the surface, with a radial growth factor $\gamma = \mathrm{d}r/\mathrm{d}t$, assumed to be constant over t. Under these conditions and $(\lambda_\beta + \lambda_\varepsilon)t \ll 1$:*

$$\text{K-40}(t) \approx \mathrm{Co}\,\gamma^3 t^3$$

$$\text{Ar-40}_r(t) \approx \frac{\lambda_\varepsilon}{4}\,\mathrm{Co}\,\gamma^3 t^4 \tag{2}$$

$$\left(\frac{\text{Ar-40}_r}{\text{K-40}}\right)_t \approx \frac{\lambda_\varepsilon}{4}\,t$$

Co is a constant containing a factor $4\pi/3$ and the number of K-40 atoms per gram of phillipsite. t can no longer be called a mineral age, but is the time elapsed since the beginning of crystal growth. However, for this discussion we use the term "apparent age" for the time one calculates from a given Ar/K ratio by application of equation (1). For the specific case considered, the "apparent age" is then $\approx\frac{1}{4}$ of the time interval elapsed since the beginning of crystal growth for a continuously growing crystal.

Equations (2) are based on an idealized model and cannot be expected to hold exactly in natural systems; the nucleus may not be of negligible volume and may contain appreciable amounts of radiogenic argon and potassium, the radial growth factor γ may change with time, the rate of accretion may be diffusion limited, etc. Such factors influence the relationship between the "apparent age" and t and in the absence of additional information limit the usefulness of equation (2) to qualitative interpretations. It is, however, interesting that the phillipsites from RIS 114P-385 and 554 cm investigated by DYMOND (1966) both have ages lower by a factor between 4 and 5 than those derived from volcanic minerals.

One of the striking features in the results is that all surface samples have "apparent ages" greater than 1 million and typically around 3 million years (Tables 7 and 8). This observation may be understood by one or more of the following concepts:

a. the phillipsites are relict minerals
b. the phillipsites have lost appreciable amounts of K
c. the phillipsites contain "inherited" argon

If phillipsites are closed systems for Ar and K and have negligible radiogenic Ar content at the beginning of their formation, then the high Ar/K ratios found in the surface samples can only mean that these minerals are old. This would introduce

---

* See appendix for derivation.

Table 7. K–Ar analyses on surface samples of phillipsites

Core	Type of sample	Sample size (mg)	Size range (μ)	K (%)	Radiogenic Ar^{40} cm^3/g × 10^7	Radiogenic Ar^{40} %	(Ar$^{40}_{rad}$/K^{40}) × 10^4	"Apparent age" 10^6 yr
AMPH 114G	N	126·056	4–10	4·64	5·54 ± 0·14	4·4	1·75 ± 0·08	3·00 ± 0·14
	N	102·882	10–37	4·98	5·55 ± 0·14	8·4	1·63 ± 0·07	2·79 ± 0·12
	N3	94·002	>37	4·60	2·8 ± 1·4	1·5	0·9 ± 0·5	1·5 ± 0·8
	M3	125·242	>37	5·32	6·83 ± 0·14	38·7	1·88 ± 0·08	3·22 ± 0·14
	M2	113·700		4·43	7·88 ± 0·13	24·8	2·60 ± 0·09	4·45 ± 0·15
	M1	87·468		2·50	9·43 ± 0·20	10·2	5·52 ± 0·17	9·42 ± 0·29*
	M3	32·082		0·4 ± 0·4	10·00 ± 0·06	6·8†		
	M2	68·392		0·4 ± 0·2	10·80 ± 0·24	5·1‡		
AMPH 113G	N	116·230	4–10	4·75	5·44 ± 0·15	4·9	1·68 ± 0·08	2·88 ± 0·14
	N	107·192	10–37	4·81	5·59 ± 0·14	7·0	1·70 ± 0·08	2·91 ± 0·14
	N3	54·095	>37	4·67	4.6 ± 1·6	1·5	1·4 ± 0·5	2·4 ± 0·9
	M3	126·135	>37	5·26	6·69 ± 0·10	37·1	1·87 ± 0·07	3·20 ± 0·12
AMPH 90	N	56·955	10–37	1·91	7·55 ± 0·79	2·1	5·8 ± 0·7	9·9 ± 1·2
PROA 172	Bulk	38·098	10–37	3·40	4·1 ± 1·2	0·4	1·8 ± 0·6	3·1 ± 1·0

N—Non magnetic.

For meaning of M_1, M_2, M_3 and N_3, see Fig. 3.

* The sample is not a pure phillipsite.

† Approximately 44% of sample weight dissolved away
‡ Approximately 32% of sample weight dissolved away
} by HCl treatment.

doubt to the concept of undisturbed pelagic sedimentation and would require erosion and redeposition of sedimentary components over wide areas of the Pacific Ocean. So far, all evidence for such mechanisms has suggested their importance on a local scale only (HEEZEN, 1959; RIEDEL, 1963). High Th concentrations and high ionium/thorium ratios in the upper sediment layers were cited as evidence for undisturbed and continuous sedimentation of phillipsite (BERNAT and GOLDBERG, 1969). However, one cannot exclude the possibility that these results reflect a recent growth about a small, but old nucleus of phillipsite.

Any loss of potassium for samples with 4·5–5·5 per cent of the element (the range given by STEINFINK, 1962) most probably is quite small. On the other hand, Amph-90 with a potassium content of the order of 2 per cent only, has the oldest "apparent age" of all the surface samples and in this case potassium loss could be invoked to explain the discrepant age. Sample Amph 114G (M1) is not pure phillipsite but contained a large amount of debris, mostly montmorillonite, and may for this reason have a high Ar/K ratio.

Inherited argon in a mineral is defined as a component of radiogenic argon which in a closed system does not derive directly from the radioactive decay of potassium, but is incorporated into the crystal during its formation. Since seawater contains a large amount of dissolved air argon, the direct incorporation of Ar-40 during phillipsite growth from solution appears unattractive. Bottom water typically has $3{\cdot}8 \times 10^{-4}$ cm^3 of argon per cm^3 of water, with an isotopic composition which is not distinguishable from that of air. If the radiogenic argon fraction extracted from a phillipsite sample of essentially zero age were one per cent of the total argon, then, as a lower limit, $3{\cdot}8 \times 10^{-6}$ cm^3 of radiogenic argon would have to be present per cm^3 of solution. Since the radiogenic argon content is more typically from 10 to 50 per cent of the total argon and a non-negligible fraction of air argon is from the extraction

Table 8. K–Ar analyses upon phillipsites from Lusiad LSDH 96

Depth (cm)	Core type	Sample size (mg)	Size range (μ)	K* (wt.%)	Radiogenic Ar† cm^3(STP)/g × 10^7	%	$\frac{(\mathrm{Ar}^{40}\ \mathrm{rad})}{(\mathrm{K}^{40})} \times 10^4$‡	"Apparent Age"§ (m.y.)	Remarks
8–11	Pilot	90·165	5–37	4·20	6·04 ± 0·10	22·6	2·10 ± 0.08	3·59 ± 0·14	
10–15	Pilot	151·428	5–37	4·95	5·76 ± 0·08	29·7	1·70 ± 0·08	2·91 ± 0·14	
	Pilot	76·410	5–37		5·76 ± 0·11	24·3			
15–18	Pilot	161·629	5–37	4·75	5·51 ± 0·13	31·6	1·70 ± 0·07	2·91 ± 0·12	
42–46	Pilot	156·810	5–37	5·05	5·31 ± 0·08	33·2	1·54 ± 0·05	2·64 ± 0·09	
20–25	Piston	174·577	5–37	5·60	6·32 ± 0·13	28·0	1·65 ± 0·07	2·83 ± 0·12	
30–35	Piston	149·880	5–37	5·16	5·64 ± 0·09	35·5	1·60 ± 0·06	2·74 ± 0·10	
	Piston	147.185	5–37		(5·7–6·0) ± 0·05	∼25			HC
50–55	Piston	91·680	5–37	5·19+	(4·4–5·1) ± 0·2	∼6	(1·2–1·4) ± 0·1	(2·1–2·4) ± 0·2	HC
		129·032	23–30	5·41	4·21 ± 0·15 ‖		1·14 ± 0·08	1·95 ± 0·14	
		103·473	23–30		4.19 ± 0·27				
		156·785	23–30		4·21 ± 0·21				
		107·130	30–37	5·29	4·56 ± 0·15	11·6	1·26 ± 0·07	2·15 ± 0·12	
		101·933	30–37	5·51	4·88 ± 0·46	2·3	1·30 ± 0·15	2·22 ± 0·26	N
		57·900	30–37	4·30	4·98 ± 0·17	4·7	1·69 ± 0·09	2·90 ± 0·15	M
		22·439	>37	4·04	5·08 ± 0·3	6·7	1·83 ± 0·16	3·13 ± 0·27	
100–105	Piston	88·500	>37	5·36+	4·47 ± 0·15	14·5	1·22 ± 0·09	2·08 ± 0·15	
	Piston	94·772	5–37	5·21	(4·3–4·9) ± 0·2	∼13	(1·2–1·4) ± 0·1	(2·0–2·4) ± 0·1	HC
151–156	Piston	140·294	5–37	5·30	(5·7–6·2) ± 0·1	∼11	(1·6–1·7) ± 0·08	(2·7–3·0) ± 0·1	HC
200–205	Piston	148·123	5–37	5·05	6·94 ± 0·08	47·2	2·02 ± 0·07	3·45 ± 0·12	
		168·840	5–37		6·97 ± 0·09	59·6			
		92·982	5–23	4·86	6·45 ± 0·12	15·5	1·94 ± 0·07	3·32 ± 0·12	
		50·655	23–30	4·76	5·37 ± 0·31	2·1	1·65 ± 0·13	2·83 ± 0·22	
		19·907	30–37	3·7 ± 0·4	5·0 ± 0·8	3·4	1·98 ± 0·25	3·39 ± 0·43	K too low
		85·471	>37	5·70+	(4·8–5·3) ± 0·12	∼15	(1·2–1·4) ± 0·08	(2–2·4) ± 0·10	HC
		53·130	5–23	0·2 ± 0·2	9·79 ± 0·38	3·7			Diss.

302–307	Piston	79·880	5–37	5·31	(5.4–5.9) ± 0.3	~8	(1·5–1·6) ± 0·1	(2·6–2·8) ± 0·2	HC
	Piston	79·888	>37	5·55	(4·0–4·5) ± 0·2	~14	(1·1–1·2) ± 0·1	(1·9–2·0) ± 0·1	HC
360–365	Piston	107·727	5–37	5·22	5·46 ± 0·13	21·3	1·53 ± 0·08	2·61 ± 0·14	
482–487	Piston	95·970	5–37	5·60	5·00 ± 0·25	8·6	1·31 ± 0·09	2·24 ± 0·22	
		136·060	23–30	5·54	5·19 ± 0·10 ‖		1.38 ± 0·05	2·36 ± 0·09	
		125·187	23–30		5·23 ± 0·12 ‖				
		125·300	30–37	5·72	4·83 ± 0·10	24·6	1·24 ± 0·05	2·11 ± 0·09	
		99·980	>37	5·71+	4·92 ± 0·11	27·2	1·25 ± 0·08	2·13 ± 0·14	
600	Core Nose	149·969	<23	5·07	6·56 ± 0·11	31·2	1·93 ± 0·08	3·30 ± 0·14	
		103·002	<23		6·69 ± 0·21	27·8			
		98·387	23–30	5·03	5·86 ± 0·18	25·4	1·71 ± 0·10	2·93 ± 0·17	
		151·585	30–37	5·24	4·60 ± 0·07	28·2	1·28 ± 0·06	2·19 ± 0·10	
		79·762	30–37		4·62 ± 0·19	9·3			
		106·080	30–37	5·90	4·29 ± 0·15	6·4	1·06 ± 0·06	1·81 ± 0·10	N
		31·993	30–37	4·22	4·91 ± 0·47	2·7	1·70 ± 0·16	2·91 ± 0·27	M
		44·690	>37	5·68	4·57 ± 0·23	8·5	1·19 ± 0·08	2·04 ± 0·14	

HC indicates hydrocarbon and chlorine contamination, making (40/36)-ratio uncertain.

Diss.: approx. 45% of bulk sample dissolved in HCl.

* K analyses marked with a cross signify use of (inferior) La, Na method, unmarked values were done by fluoboric-boric acid method or mass spectrometry.

† Error is calculated from maximum possible uncertainty in Ar^{40}/Ar^{36} ratio.

‡ Error is sum of relative errors in Ar and K. A 2% error has been assumed for K analyses by mass spectrometric and fluoboric-boric acid method, 4% for La, Na borate method and 3% for pairs determined by both methods.

§ $\lambda_e = 0{\cdot}585 \times 10^{-10}\,\mathrm{yr}^{-1}$, $\lambda_\beta = 4{\cdot}72 \times 10^{-10}\,\mathrm{yr}^{-1}$, $K^{40}/K = 1{\cdot}19 \times 10^{-4}$ (assuming K in phillipsite is not fractionated).

‖ Extracted in multiple steps.

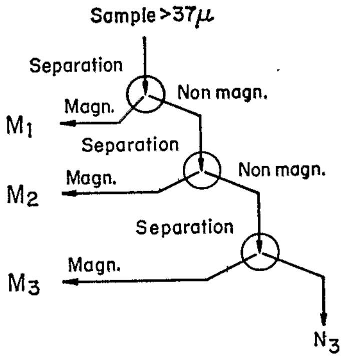

Fig. 3. Symbolical description of sample separation for > 37 μ fraction.

system, the above amount of dissolved radiogenic argon is most conservative. No process can be imagined which would keep such an enormous excess of gas confined in a volume of water over long periods of time.

Any inherited argon therefore must derive from impurities, either in the form of a detrital particle from which phillipsite growth starts, or as absorbed particles, forming an inclusion later on. Microphotographs or scanning electron micrographs such as those shown in Fig. 4 may give some justification for such an explanation. Why such impurities should lead to "apparent ages" in the neighborhood of 3 million years in samples as widely separated as shown in Table 2 is a puzzle.

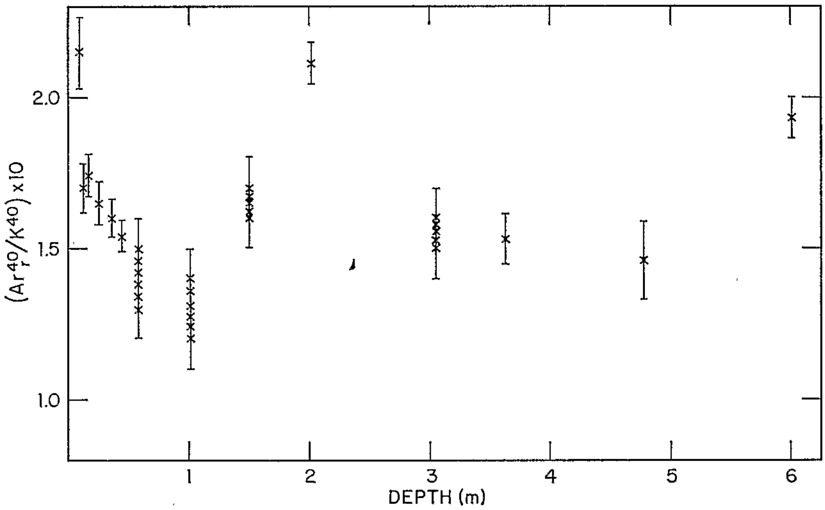

Fig. 5. Variation of Ar-40/K-40 ratio with depth for LSDH 96, 5–37 μ size fraction.

The "apparent ages" of phillipsites deeper in the deposits (core LSDH 96; Table 8) show variations of the ages not only with depth but also with grain size. In general, the larger size fractions have smaller "apparent ages". The "apparent ages" for the 5–37 μ fraction oscillate between about 3·6 × 10^6 and 2 × 10^6 yr (Fig. 5). The > 37 μ fraction, however, is almost constant below 55 cm and up to 600 cm at 2 × 10^6 yr. The only exception is found at the 50–55 cm level where this fraction

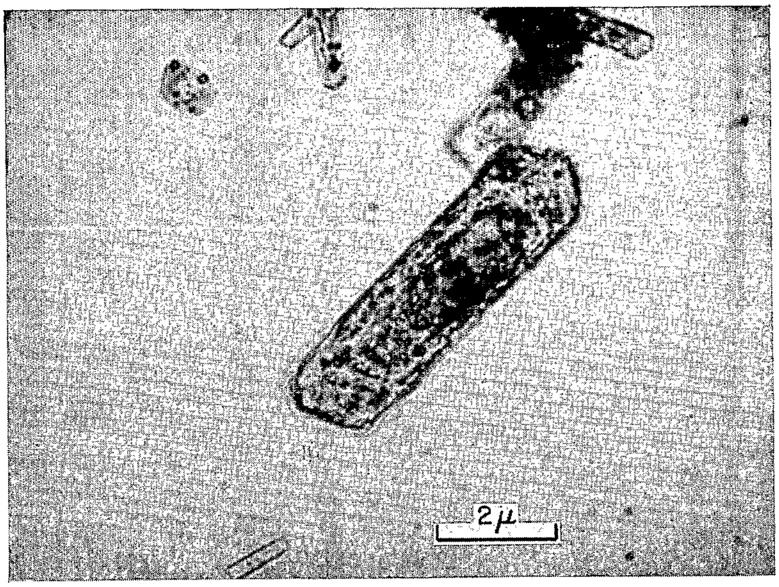

Fig. 4a. Microphotograph of marine phillipsite showing zones of inclusions. (Photo courtesy of Dr. R. A. Sheppard, U.S.G.S.)

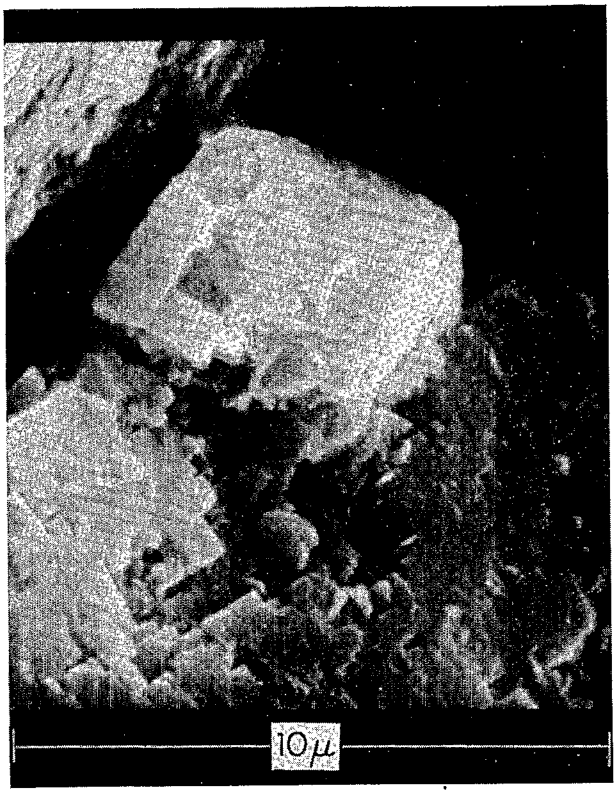

Fig. 4b. Scanning electron micrograph of 30–37 μ phillipsite isolate from 600 cm in LSD H 96. Note inclusion in lower central area. 10,000 × (Photo courtesy of Dr. William Ferguson, Marathon Oil Co.)

has an unusually high (compared with the results from other size fraction at this level) Ar/K ratio. The variation of the Ar/K ratio with grain size is especially evident in the samples from the 600 and 200 cm level (the potassium analysis of 30–37 μ size fraction from 200 cm is probably in error). At the 485 cm level, however, the variation is very small.

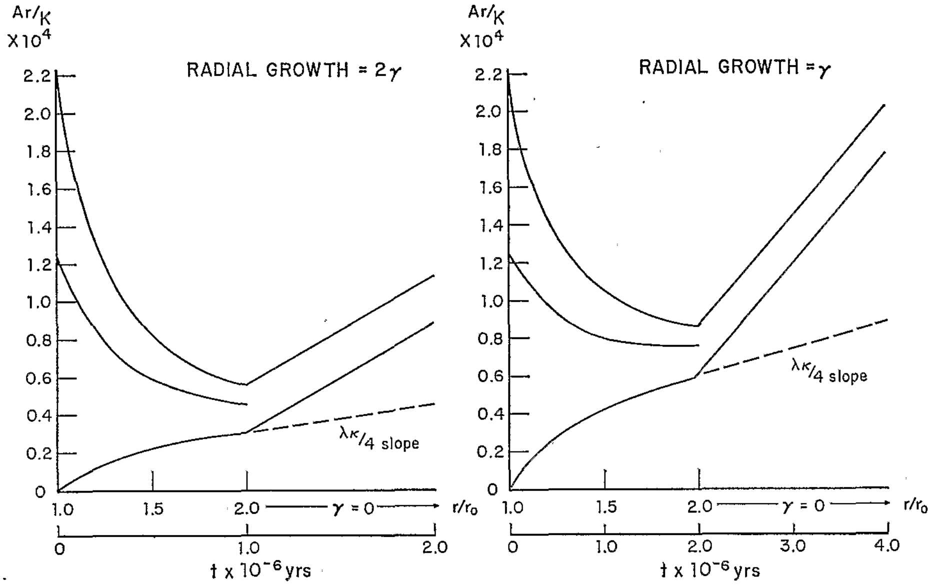

(a) (b)

Fig. 6a,b. Calculated $\text{Ar-40}_{\text{rad}}/\text{K-40}$ ratios for spherical growth from r to $2r$ and varying amounts of argon at the "beginning of growth" ($r/r_0 = 1$). The initial argon does not have to be "inherited" in the usual sense, but may have been incorporated during an earlier period of growth. In addition to the change of $\text{Ar-40}_{\text{rad}}/\text{K-40}$ during growth, the figures also show the increase of this ratio after growth has ceased.

Although one cannot rule out the occurrence of diffusive argon losses with certainty, there is enough evidence in the data to show that they are of minor importance. If the sharp decrease in the Ar/K ratios for the first 100 cm of sediment were due to loss of radiogenic argon, it is difficult to understand how the phillipsites in the adjacent 100 cm could retain their argon so well. The increase of this ratio with decreasing grain size also rules against diffusive argon losses.

Continued crystal growth may provide an explanation. In Fig. 6, equations (2) have been applied to the more general case of growth from a nucleus of radius r to $2r$ for two different growth factors, γ and 2γ, and with an amount of radiogenic argon at $t = 0$ reflected by the value of the Ar/K ratio at the beginning of growth. The curves show a decreasing Ar/K ratio with increasing radius or time ($r = \gamma t$) up to $2r$ in the presence of "inherited" argon. For the larger radii, the slope of the curves reaches an asymptotic value of $\lambda_\varepsilon/4$. Beyond $2r$, $\gamma = 0$ has been assumed and Ar/K increases with slope λ_ε. Although the details of the model clearly can be changed for a variety of conditions, its general solutions offer the simplest explanation of the trend observed between 0 and 200 cm in Fig. 5. We abstain from an interpretation of the results below 200 cm because this would require additional hypotheses.

A test for the growth hypothesis over long time intervals may be derived in the following way: an ideal nongrowing crystal has a uniform Ar/K ratio throughout its volume, while this ratio in a growing crystal is a function of its radial position. Using the same approximation and assumptions as before, one finds for the Ar/K ratio in a core of radius $r_1 = \gamma t_1$

$$\frac{\text{Ar-40}_r}{\text{K-40}} \approx \lambda_\varepsilon \left[(t - t_1) + \frac{t_1}{4}\right].$$

Removal of the outer portions of a spherical growth would result in

$$\lambda_\varepsilon t > \frac{\text{Ar-40}_r}{\text{K-40}} > \frac{\lambda_\varepsilon}{4} t$$

and would be governed by the particular amount of outer shell removed. For example, the case of $r_1 = 1/2r$ gives a ratio of Ar/K of $\lambda_\varepsilon 5t/8$. Since we have assumed that $\lambda_\varepsilon t \ll 1$, only the concentration of argon is changing.

This can now be compared with the results from the chemically treated samples (AMPH 114 G-M2 and -M3 and LSDH 96-200). After etching the outer portions away with HCl, the argon concentrations are substantially higher. As expected, nearly all of the potassium is lost in the dissolution, but if the original amount is used, the ratios change in the right direction. Since we have no insight into the details of the HCl treatment on the phillipsite crystals, this must be regarded as a possible but tentative interpretation.

Similarly, the observed variation in the Ar/K ratios with grain size can be explained by a continuously growing mineral within the deposits. For one reason or another, the smaller crystals have not accreted additional material and new nucleation does not occur. Hence they have higher Ar/K ratios than their growing counterparts. While it is also possible that this simply reflects a relatively higher contribution of an inherited contaminant in the small crystals, no contradiction to the growth hypothesis results as this trend is preserved (see Fig. 5) and the Ar/K ratio for the 600 cm sample is too low. The abnormally high Ar/K ratio in LSDH 96-50 cm for the $>37\ \mu$ size class is not as yet understood.

Magnetic separates of the phillipsites revealed a most unusual set of results. The more magnetic fractions had older ages, i.e. higher values of the Ar-40/K-40 ratio for a given level. This observation was initially made on the surface samples AMPH 113G and AMPH 114G and subsequently on 2 separates from LSDH 96 (50 and 600 cm). Although there are no consistent changes in the potassium concentration as a function of magnetic properties of the separates, the trends in the Ar/K ratios are found in all of the samples so far analyzed. This phenomenon is almost certainly related to the existence of inherited argon by incorporation of solids. The more magnetic or higher iron containing samples also were able to accommodate more argon during the early stages of formation. A correlation between uranium concentrations and magnetic properties due to inclusions with high susceptibility has been observed by Arrhenius and Korkisch (1959).

SUMMARY

A model for the growth of phillipsite in the marine sedimentary column is proposed to account for the complex variations in the apparent K–Ar ages and for the variations in the concentrations of uranium and thorium and of their isotopes with depth.

Phillipsites are presumed to nucleate about relict minerals (and perhaps also to occlude them during growth). Such minerals, if they contain appropriate amounts of argon, can account for the non-zero ages of the surface phillipsites.

The crystals of phillipsite, growing within the column, accommodate potassium in the absence of the daughter argon. On such a basis the initial decrease in the K–Ar apparent age with depth can be explained. Also, the decreases in the uranium and thorium and the increases in phillipsite concentrations with depth are explicable.

The subsequent increase in the Ar-40/K-40 ratio with depth describes a situation in which the addition of Ar by K-40 decay overcompensates the dilution of the Ar by the addition of crystal formation.

Our model for the systematics of growth is clearly overschematized but does provide a background on which to discuss the Ar/K ratios both as a function of depth, grain size and magnetic properties of the isolate. In any case, the phillipsites cannot be dated by the K–Ar method in a straightforward simple way. Perhaps, an extrapolated age based upon apparent ages of continuously dissolved samples (peeling off layers by layers) might be a reasonable way to use K–Ar geochronology.

Acknowledgment—This work has been carried out with the support of the U.S. Atomic Energy Commission, Division of Biology and Medicine, under Grant AT(11-1) 34, Project 84. Miss MARY TIFFANY assisted with some of the potassium analyses.

REFERENCES

ARRHENIUS G. and KORKISCH H. (1959) Uranium and thorium in marine minerals. Intern. Oceanog. Congr. Preprints 497, (editor M. Sears). Amer. Assoc. Adv. Sci., Washington D.C.

BERNAS BEDRICH (1968) A new method for decomposition and comprehensive analysis by atomic absorption spectrometry. *Anal. Chem.* **40**, 1682–1686.

BERNAT M. and GOLDBERG E. D. (1969) Thorium isotopes in the marine environment. *Earth Planet. Sci. Lett.* **5**, 308–312.

BIERI R. H., DYMOND J. D. and KOIDE MINORU (1968) A high temperature ultra high vacuum furnace for gas extraction from geologic samples. *Earth Planet. Sci. Lett.* **1**, 395–396.

BIERI R. H. and KOIDE MINORU (1968) Valve for precise pipetting of small amounts of gases. *Rev. Sci. Instrum.* **38**, 1159–1160.

BONATTI E. (1963) Zeolites in Pacific pelagic sediments. *Trans. N.Y. Acad. Sci.* **25**, 938–948.

DEER W. A., HOWIE R. A. and ZUSSMAN J. (1963) *Rock-Forming Minerals. Vol.* 4. *Framework Silicates*, pp. 387–388. John Wiley.

DYMOND J. (1966) Potassium–argon geochronology of deep sea sediments. *Science* **152**, 1239–1241. See also DYMOND J. D. (1966) Potassium–argon geochronology of deep-sea sedimentary material. Thesis Scripps Institution of Oceanography, University of California at San Diego, La Jolla, California.

GOLDBERG E. D., KOIDE M., GRIFFIN J. J. and PETERSON M. N. A. (1964) A geochronological and sedimentary profile across the North Atlantic Ocean. In *Isotopic and Cosmic Chemistry*, (editor H. Craig, S. L. Miller and G. J. Wasserburg), pp. 211–232. North-Holland.

GOLDBERG E. D. (1961) Chemical and mineralogical aspects of deep-sea sediments. *Phys. Chem. Earth* **4**, 281–302.

GOLDBERG E. D. (1963) Mineralogy and chemistry of marine sedimentation. In *Submarine Geology*, 2nd edition (editor Francis P. Shepard), pp. 436–466. Harper & Row.

Hay R. L. (1966) Zeolite, and zeolitic reactions in sedimentary rocks. *Geol. Soc. Amer. Spec. Paper* **85,** 130 pp.

Heezen B. C. (1959) Dynamic processes of abyssal sedimentation: erosion, transportation and redeposition on the deep-sea floor. *Geophys. J., Roy. Astron. Soc.* **2,** 142–163.

Lanphere M. A. and Dalrymple G. B. (1967) K–Ar and Rb–Sr measurements on P-207, the U.S.G.S. interlaboratory standard muscovite. *Geochim. Cosmochim. Acta* **31,** 1091–1094.

Murray J. and Renard A. F. (1891) *Deep-Sea Deposits.* Reports Challenger Expedition, London.

Riedel W. R. (1963) The preserved record: paleontology of pelagic sediments. *The Sea,* Vol. 3, pp. 866–887. Interscience.

Sheppard R. A. and Gude A. J. 3rd (1968) Distribution and genesis of authigenic silicate minerals in tuffs of Pleistocene Lake Tecopa, Inyo County, California. *U.S. Geol. Surv. Prof. Paper* **597,** 38 pp.

Somayajulu B. L. K. and Goldberg E. D. (1966) Thorium and uranium isotopes in sea water and sediments. *Earth Planet. Sci. Lett.* **1,** 102–106.

Steinfink H. (1962) The crystal structure of the zeolite phillipsite. *Acta Crystallogr.* **15,** 644.

Tosto S. (1948) La phillipsite del centro vulcanicò di Agnone, nei pressi di Augusta prov. Sir acusa (Nuovo giacimento). *Boll. Accad. Gioenià Sci. Nat. Catanià Ser.* **4,** No. 1, 32 pp.

APPENDIX

For a spherical object of surface $4\pi r^2$ and radial growth rate $\gamma = \mathrm{d}r/\mathrm{d}t$ = constant, the volume increase per unit time, if growth starts from a nucleus of negligible volume ($\gamma = r/t$), is given by

$$\frac{dV}{\mathrm{d}t} = 4\pi r^2 \frac{\mathrm{d}r}{\mathrm{d}t} = 4\pi\gamma^3 t^2.$$

Thus, if ρ is the density and $n_k{}^{40}$ the number of K-40 atoms per gram, then the change in potassium due to growth is

$$\left(\frac{\mathrm{d}K}{\mathrm{d}t}\right)_{\text{growth}} = 4\pi\gamma^3 t^2 \rho n_k{}^{40} = C_1\gamma^3 t^2$$

where $C_1 = 4\pi\rho n_k{}^{40}$.

To find the net change, the number of K-40 atoms removed by radioactive decay must be considered also. However, since the number of decaying K-40 atoms per unit time is always $<$ $(4\pi/3)\,\rho n_k{}^{40}\gamma^3 t^3(\lambda_\beta + \lambda_\varepsilon)$ and

$$\frac{\text{Rate of decaying K-40}}{\text{Rate of K-40 added}} < \frac{t}{3}(\lambda_\beta + \lambda_\varepsilon) = 1{\cdot}77 \times 10^{-10}t$$

the loss for the times short with respect to a billion years is neglected.

$$\text{K-40}(t) = \frac{4\pi}{3}\rho n_k{}^{40}\gamma^3 t^3 = \text{Co}\,\gamma^3 t^3$$

Since

$$\frac{\mathrm{dAr\text{-}40}_r}{\mathrm{d}t} = \lambda_\varepsilon\text{K-40} = \lambda_\varepsilon\text{Co}\,\gamma^3 t^3$$

$$\text{Ar-40}_r(t) = \frac{\lambda_\varepsilon}{4}\,\text{Co}\,\gamma^3 t^4$$

or

$$\frac{\text{Ar-40}_r}{\text{K-40}} = (\lambda_\varepsilon/4)t.$$

At some radius $r_1 < r$, argon and potassium concentrations are determined by

$$\text{Ar-40}_r(t) = \frac{\lambda_\varepsilon}{\lambda_\beta + \lambda_\varepsilon}[\text{K-40}(t_1) - \text{K-40}(t_1)e^{-(\lambda_\beta+\lambda_\varepsilon)(t-t_1)}] + \text{Ar-40}_r(t_1)$$

$$\text{K-40}(t) = \text{K-40}(t_1)e^{-(\lambda_\beta+\lambda_\varepsilon)(t-t_1)}$$

and

$$\frac{\text{Ar-40}_r(t)}{\text{K-40}(t)} \approx \lambda_\varepsilon \left[(t - t_1) + \frac{t_1}{4}\right]$$

while K-40 and Ar-40 in the shell $r > r_1$ are determined by

$$\text{K-40}(t) = \text{Co}\gamma^3(t^3 - t_1{}^3)$$

$$\text{Ar-40}_r(t) = \lambda_\varepsilon \text{Co}\,\gamma^3 \left[\frac{t^4}{4} - \frac{t_1{}^4}{4} - t_1{}^3(t - t_1)\right].$$